Microwave Processing of Starch-Based Porous Structures for Tissue Engineering Scaffolds

Fernando G. Torres,[1] Aldo R. Boccaccini,[2] Omar P. Troncoso[1]

[1]*Polymers and Composites Group, Catholic University of Peru, Lima 32, Peru*
[2]*Department of Materials and Centre for Tissue Engineering and Regenerative Medicine, Imperial College London, London SW7 2BP, United Kingdom*

Received 13 March 2006; accepted 24 August 2006
DOI 10.1002/app.25345
Published online in Wiley InterScience (www.interscience.wiley.com).

ABSTRACT: A novel microwave (MW) processing technique was used to produce biodegradable scaffolds for tissue engineering from different types of starch-based polymers. Potato, sweet potato, corn starch, and nonisolated amaranth and quinoa starch were used to produce porous structures. Water and glycerol were used as plasticizers for the different types of starch. Characterization of the pore morphology of the scaffolds was carried out with scanning electron microscopy. Three-dimensional structures with variable porosity and pore size distribution were obtained with the MW foaming technique. The amount of remaining water in the scaffolds and their corresponding densities showed important variations among the different types of starch. Compressive mechanical properties were assessed by indentation tests, and a strong dependence of the indentation stress on the average pore size was found. Studies in simulated body fluid were used to assess the *in vitro* bioactivity, degradability, and surface topology evolution in the scaffolds. © 2006 Wiley Periodicals, Inc. J Appl Polym Sci 103: 1332–1339, 2007

Key words: biological applications of polymers; biomaterials; macroporous polymers

INTRODUCTION

Tissue engineering (TE) is a challenging multidisciplinary field that seeks to replace or repair natural tissues by the manipulation of cells by different methods. One method is the use of biodegradable polymeric scaffolds. TE scaffolds should provide a surrogate structure for the extracellular matrix. Therefore, scaffolds must carry out the functions of the native extracellular matrix. This imposes some desired characteristics on TE scaffolds that have to be addressed with the choice of adequate materials and manufacturing methods.

Among the different types of TE scaffolds that have been reported in the literature, foamed structures have received considerable attention in recent years.[1] Foams were developed because of the need for more surface area and a more enclosed structure compared to the early fiber-mesh-type scaffolds.

Some of the different manufacturing techniques reported for the development of polymeric TE scaffolds included phase separation and freeze drying,[1,2] particulate leaching,[3,4] and CO_2-based foams.[5] There has been an increasing need for the development of new manufacturing techniques for TE scaffolds to cope with the changing demands in the field. Improved control of porosity (P) and pore size distributions are some of the challenges.[6]

Another important requirement for TE scaffolds is bioactivity. *In vitro* bioactivity is evaluated by the soaking of the scaffold in a solution able to reproduce *in vivo* surface-structure changes. The simulated body fluid (SBF) formulated by Kokubo et al.[7] has ion concentrations and pH values almost equal to those of human blood plasma and is considered useful for a qualitative measure of bioactivity.[8,9]

Natural biodegradable polymers, such as collagen,[10,11] fibrinogen,[12,13] chitosan,[14] and starch,[15] have been used in the past for the production of TE scaffolds. Starch is composed of anhydroglucose units, which form two different polymers: the linear amylose and the branched amylopectin. Amylose comprises 20–30% of the starch granule and consists of long chains of α-(1,4)-linked D-glucose units with a degree of polymerization ranging[16] from 3×10^2 to 1×10^4. On the other hand, amylopectin comprises 70–80% of the granule and has α-(1,4)-linked glucose chains joined by 1,6 linkages with a degree of polymerization[17] of about 10^8.

Amylose and amylopectin form helical segments, which pack together to give crystalline regions that can be observed under polarized light as a Maltese cross on the starch granules. When heated, starch

Correspondence to: F. G. Torres (fgtorres@pucp.edu.pe) or A. R. Boccaccini (a.boccaccini@imperial.ac.uk).

Contract grant sponsor: Royal Society (for F.G.T.'s research at Imperial College).

undergoes a process known as *gelatinization*, where the granules swell, leach amylopectin, and lose birefringence.[18]

The structure of starch can be also modified by crosslinking, which is performed by the treatment of granular starch with chemical agents such as sodium trimetaphosophate,[19] epichlorophydrin,[20] phosphoryl chloride,[21] formaldehyde,[22] and anhydride combinations[22] (adipic acid and citric/acetic acid). Crosslinking provides the starch with improved resistance to processing conditions such as temperature, acid, and shear. Pure natural starch molecules are not expected to form crosslinks during microwave (MW) heating.

Recently, Sjöqvist and Gatenholm[23] used MW processing for the production of starch-based foams for packaging applications. A potato starch–water dispersion was microwaved and created an amorphous material with irregular and large pores. The pore-forming ability of potato starch was studied, and the inherent properties of the polymers, rather than the organization of the granules, were found to determine the foaming process.

Malafaya et al.[24] used the MW technique to produce porous starch-based materials for drug delivery. Material properties and structural characterization data were reported along with their degradation in an aqueous media.

In this study, a new microwave foaming (MWF) technique was developed to produce biodegradable three-dimensional porous scaffolds for TE from different types of starch-based polymers. To our knowledge, no previous attempts have been made to manufacture highly porous foams for TE scaffolds by this MWF technique. The pore size distribution, P, and density were measured to characterize the foam structure, and indentation tests were carried out to assess the mechanical properties. *In vitro* bioactivity and degradation were also studied by immersion in SBF.

EXPERIMENTAL

Materials

Potato, sweet potato, corn, and nonisolated amaranth and quinoa starch, which were industrial food grade, were used. Starch powder was first mixed with water and plasticizers and heated in a water bath at 70°C to gelatinize the starch and allow the amylose chains to leave the starch granules and form a gel.[25,26]

The gelatinized mixtures were then placed in heat-resistant (MW-resistant) polypropylene containers and microwaved for controlled times in a commercial Miray MW oven (Shunde, China) with heating power of 800 W and a frequency (f) of 2450 MHz.

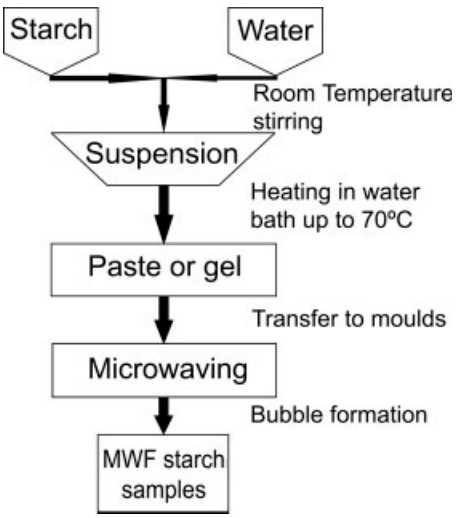

Figure 1 Manufacturing route for the preparation of microwaved starch scaffolds.

Trials with ungelatinized starch suspensions were also carried out. However, the formation of cells was highly inhomogeneous, and powdery starch regions were found in several parts of the foam. Figure 1 depicts the manufacturing route used for the preparation of the microwaved starch foams.

Characterization techniques

Stereomicroscopy was used to characterize features, such as pore morphology and dimensions, at the mesoscale.[27,28] The morphology and microstructure of the inner cores of the scaffolds were characterized with scanning electron microscopy (SEM; Jeol JSM, Tokyo, Japan). Small pieces of the specimens were mounted onto stubs with adhesive tape and sputtered with a gold layer. Accelerating voltages in the range 6–18 kV were used for the observation of cross-sections.

Differential scanning calorimetry (DSC) experiments were carried out in a PerkinElmer Pyris DSC-7 calorimeter (Wellesley, MA). Scanning rates of 10°C/min were used in the temperature range 20–200°C. The moisture content of the specimens was determined in a PerkinElmer Pyris TGA7 thermogravimetric analyzer at a scanning rate of 20°C/min.

The apparent density of the foams (ρ) was determined by measurement of the volume and mass of cubic foam specimens (nominally, $5 \times 5 \times 5$ mm^3). Measurements of the overall dimensions were taken with vernier calipers (across 20 samples per composition). A theoretical P was calculated by comparison of ρ to the density of the nonporous material (ρ_o) according to eq. (1):

$$P = 1 - \frac{\rho}{\rho_o} \quad (1)$$

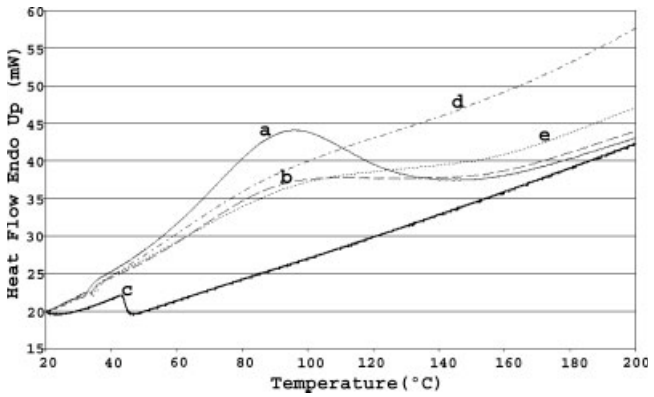

Figure 2 DSC curves for (a) potato, (b) corn, (c) sweet potato, (d) amaranth, and (e) quinoa native starch. Gelatinization peaks are present only for starches.

The amount of water evaporated during bubble formation was estimated by weighing of the water–starch suspension before water-bath heating ($Weight_{mixture}$) and of the foam after processing ($Weight_{foam}$). These weights and the percentage of starch in the mixture (% Starch) were used to calculate the remaining water content (RWC) according to eq. (2):

$$\text{RWC}\ (\%) = \frac{\text{Weight}_{\text{Foam}} - \text{Weight}_{\text{Mixture}} \times \%\ \text{Starch}}{\text{Weight}_{\text{Foam}}} \quad (2)$$

Compressive mechanical properties were assessed by indentation tests. These tests were carried out with a Check-Line HPSDO (New York) durometer according to ASTM D 2240,[29] which is prescribed for the determination of hardness of soft materials (e.g., rubbers, cellular plastics, gel-like materials). An indenter with a diameter of 2.38 mm was used. The stress (MPa) needed to produce a 1-mm indentation in the specimens was recorded. Three repetitions were carried out for each sample.

In vitro bioactivity studies were carried out with SBF on the basis of the formulation and method developed by Kokubo et al.[7] The specimens were attached to a cover glass and placed in 24-well plates with tweezers; subsequently, an aliquot (2 mL) of SBF (37.8°C) was added to them. During the immersion period, the samples were kept at 37.8°C in a humidified incubator, and the SBF was refreshed after 6 h of incubation and then after 24 h, 48 h, and every 3 days after incubation. The specimens were then collected after 1, 3, 7, 14, and 21 days of incubation. The samples were rinsed in distilled water three times, vacuum-dried for 3 h, and finally stored in desiccators for further examination.

The temperature and pore size evolution was assessed by heating of the samples for 15, 45, 60, 75, 90, 105, 120, 135, and 150 s to obtain information about pore size and local temperature as a function of time. An IR Lutron TM-2000 thermometer (Taipei, Taiwan) performed surface temperature measurements immediately after each MW heating cycle was completed.

RESULTS AND DISCUSSION

Thermal analysis (DSC) of the unprocessed polymers

Figure 2 shows representative DSC curves for the different types of starch used in the experiments. All specimens were tested with the original moisture contents at room temperature. These moisture contents were in the range 12–14% in all cases as determined by thermogravimetric analysis. Potato starch showed the largest gelatinization peak in the range 60–130°C. This was in agreement with previous data from the literature.[30] Corn starch and nonisolated quinoa starch showed similar gelatinization behaviors, described by smaller peaks in the same temperature range as potato starch. Sweet potato starch and nonisolated amaranth starch, by contrast, showed almost no gelatinization peaks.

Morphology of the foams

Cross-sections of scaffolds are depicted in Figure 3. Figure 3(a) shows the SEM micrograph of corn starch foam. Open and interconnected pores that were not uniform in size and did not have a particular shape or orientation were found. A sweet potato starch scaf-

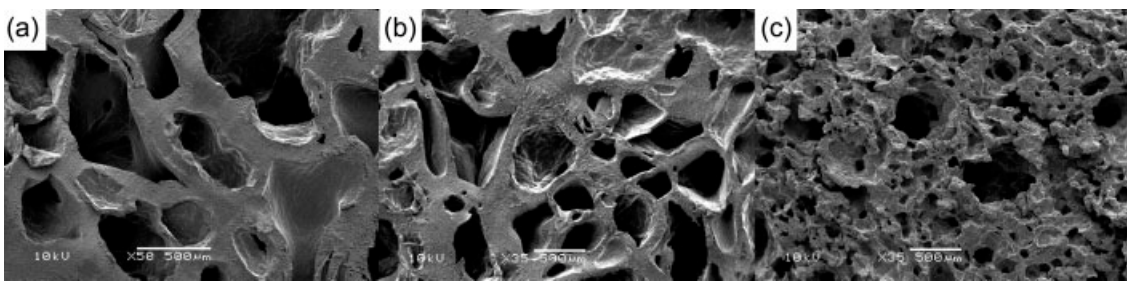

Figure 3 SEM micrographs showing the microstructure of a (a) 40% corn starch/60% water, (b) 40% sweet potato starch/60% water, and (c) 51% soy/42% water/7% glycerin scaffolds.

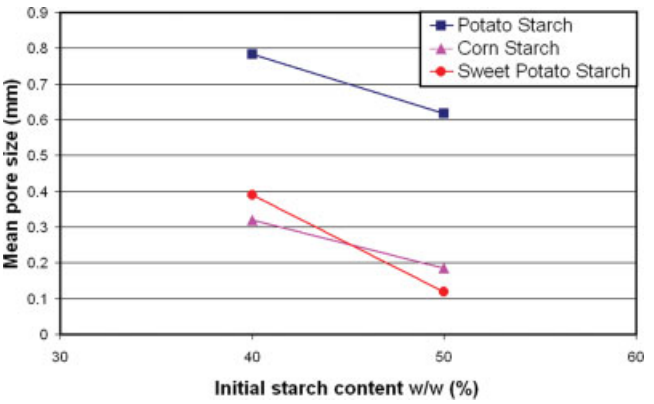

Figure 4 Variation of mean pore size with initial starch content for different sources of starch. [Color figure can be viewed in the online issue, which is available at www.interscience.wiley.com.]

fold is shown in Figure 3(b). As in the corn starch scaffolds, the open pores had different shapes and sizes. The soy flour foamed structure is shown in Figure 3(c). A more uniform pore size distribution was observed, with pores formed by closed cells and thick walls.

Foams based on potato, corn, and sweet potato starch were prepared with two initial concentrations of starch (40 and 50 wt %). Potato starch foams had the widest pore size distribution, which ranged from 100 μm to 1.8 mm, whereas corn and sweet potato starches produced unimodal asymmetric distributions with pores ranging from 100 μm to 1 mm.

Figure 4 depicts the dependence between the initial starch content and the mean pore size. In all cases, higher starch contents corresponded to smaller pores. The mean pore sizes of corn-starch-based foams were 0.3 mm at 40% and 0.2 mm at 50%, whereas for sweet potato starch foams, pore size values were 0.4 mm at 40% and 0.1 mm at 50%. On the other hand, potato starch foams showed significantly larger pores than the other types (0.8 mm at 40% and 0.6 mm at 50%).

Overall ρ and *P*

Corn starch scaffolds showed the highest densities compared to potato- and sweet-potato-based scaffolds. Lower densities in the other types of scaffolds were accompanied by lower RWC values, larger pores, and higher overall *P* values. As shown in Table I, potato starch foams had the highest *P* values (80–87%), whereas corn starch scaffolds had the lowest *P* value (≈ 62%).

The density of the foams is shown in Figure 5 for three concentrations of initial starch content (30, 40, and 50%). No significant difference was found for sweet potato and corn starch foams, although corn starch samples with a concentration of 50% had a slightly higher density value (≈ 0.6 g/cm^3) than the samples with a concentration of 40% (≈ 0.55 g/cm^3). The dependence between potato starch content and the density of the produced foam was observed as the highest density values (≈ 0.3 g/cm^3) and were obtained with the lowest concentrations (30%), whereas for 50% potato starch, the density was 0.2 g/cm^3.

A linear tendency between the initial potato starch content and RWC in shown in Figure 6. The negative slope showed that as the initial starch content increased (from 30 to 50%), RWC decreases (from 25 to 10%) because at higher starch concentrations, there was less water to be evaporated by the process. This was also true for sweet potato and corn starches, but the linear tendency was not repeated.

Indentation tests of dry foams

Indentation is related to the compressive collapse strength of open-cell foams because of the lack of sideways expansion as the foam cells collapse when

TABLE I
ρ and *P* Values for Different Sources of Starch

Specimen	ρ_o (g/cm^3)[41–45]	ρ (g/cm^3)	Calculated average *P* (%) from eq. (1)	RWC (%)
50% potato starch/50% water	1.472	0.191 ± 0.017	87.1	10
40% potato starch/60% water	1.472	0.229 ± 0.061	84.5	14
30% potato starch/70% water	1.472	0.303 ± 0.021	79.4	24
50% corn starch/50% water	1.450	0.623 ± 0.174	57.0	22
40% corn starch/60% water	1.450	0.583 ± 0.071	62.9	23
30% corn starch/70% water	1.450	0.55 ± 0.05	62.0	25
50% sweet potato/50% water	1.5	0.472 ± 0.042	68.5	12
40% sweet potato/60% water	1.5	0.462 ± 0.056	69.2	5
30% sweet potato/70% water	1.5	0.373 ± 0.027	75.2	32
30% amaranth/70% water	1.369	0.379 ± 0.024	72.3	
20% amaranth/70% water	1.369	0.243 ± 0.056	82.25	
51% soy/42% water/7% glycerine	1.25	0.506 ± 0.069	59.52	
41% soy/50% water/9% glycerine	1.25	0.375 ± 0.053	70	

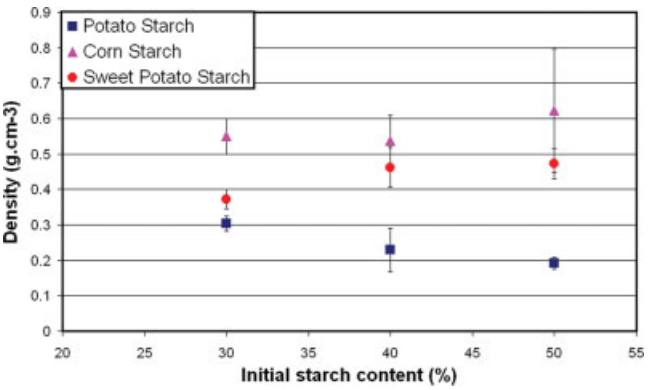

Figure 5 Variation of density with initial starch content for different sources of starch. [Color figure can be viewed in the online issue, which is available at www.interscience.wiley.com.]

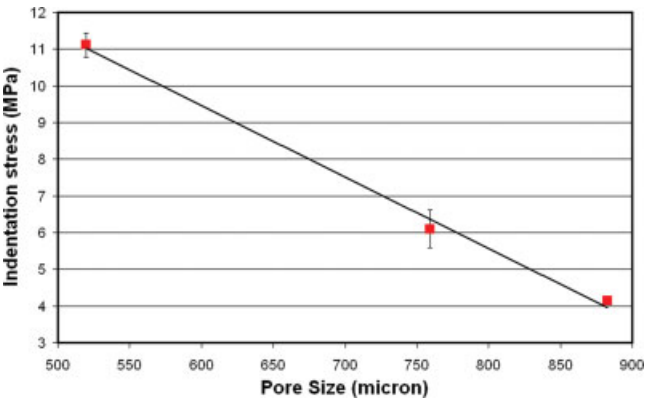

Figure 7 Changes in indentation stress versus mean pore size for potato-based scaffolds. [Color figure can be viewed in the online issue, which is available at www.interscience.wiley.com.]

they are compressed. Thus, for foams with P values higher than about 70%, the indentation pressure could be considered equal to the compressive plastic-collapse strength (σ^*_{pl}),[31] which is expressed by eq. (3):

$$\sigma^*_{pl} \approx 0.3\sigma_{ys}\left(\frac{\rho}{\rho_o}\right)^{3/2} \quad (3)$$

where σ_{ys} is the yield strength of the solid material and ρ/ρ_o is the relative density of the foam.

A strong dependence of indentation stress on the average pore size was found (see Fig. 7). Lower indentation pressures were obtained for specimens with larger pores for a constant-shape indentor. This was because σ^*_{pl} depended on the relative density [see eq. (4)] and specimens with large pores had lower relative density values than foams with smaller pores.

A linear decreasing tendency (slope = −0.0194) between indentation pressure and mean pore size is shown in Figure 7. For a mean pore size of 500 μm, the indentation pressure was 11 MPa. For larger mean pore sizes (750 and 900 μm), the indentation pressures were 6 and 4 MPa, respectively.

Theoretical analysis of MW heating and bubble formation during the MWF process for starch-based polymers

MW heating is usually defined as volumetric heating[21] and is believed to occur from inside out. A relevant material property in MW heating is the complex permittivity (ε^*), which is given by eq. (4):

$$\varepsilon^* = \varepsilon' - j\varepsilon'' \quad (4)$$

where ε' is the permittivity of the material and ε'' is the loss factor (j indicates the imaginary unit). ε' measures the ability of the material to store electromagnetic radiation, and ε'' measures the ability of the material to dissipate electrical energy into heat.

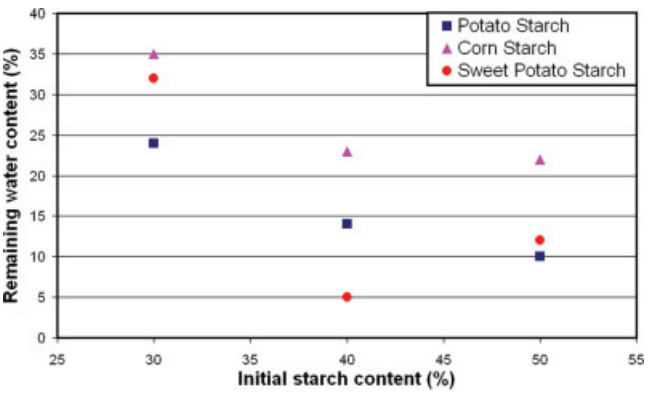

Figure 6 RWC in the microwaved specimens calculated with eq. (2) and expressed as a percentage of the final foam weight. [Color figure can be viewed in the online issue, which is available at www.interscience.wiley.com.]

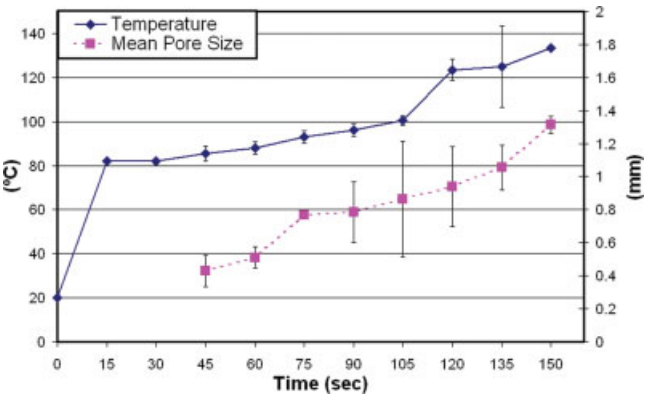

Figure 8 Variation of superficial temperature and mean pore size with time for 50% potato starch/50% water scaffolds. [Color figure can be viewed in the online issue, which is available at www.interscience.wiley.com.]

TABLE II
Specimen Weights Before and After the SBF Immersion Tests

Specimen	Dry weight before SBF (g)	Soaked weight in SBF (g)	Soaked weight in deionized water (g)	Dry weight after SBF (g)
40% corn starch/60% water	0.562	1.554	1.532	0.499
40% potato starch/60% water	0.452	3.055	2.609	0.304
40% sweet potato starch/60% water	0.558	3.730	3.678	0.568
51% soy/42% water/7% glycerine	0.582	—	—	—
20% amaranth/80% water	0.585	—	—	—

Therefore, the dissipated power during MW heating depends on the value of ε'', the permittivity of free space (ε_0), and the properties of the MWs, namely, f and the electrical field strength (E_{rms}):

$$P = 2\pi f \varepsilon_0 \, \varepsilon'' E_{rms}^2 \quad (5)$$

During the heating stage, ε'' is not constant but is dependent on moisture content and temperature.[32] Starch behavior under MW radiation has been studied elsewhere,[33] and no significant difference in the dielectric properties was detected between different types of starch–water solutions (potato, corn, and wheat starch). The important factor was found to be the water content.

Some forms of radiation, such as γ irradiation, cause chemical modifications in the starch.[34,35] However, due to the fact that MW radiation contains only 1 J/mol of photons, it is generally accepted that in the absence of other chemical agents, no significant modification is to be expected during MW heating.[36]

The heating rate was assessed by measurement of the superficial temperature and mean pore size evolution (Fig. 8). For the first 15 s, the temperature increased abruptly (from room temperature to 80°C). After that, it still grew but at a lower rate until it passed the water boiling point. Then, the temperature rapidly increased to 120°C and finally started steadily rising until the end of the process. As the surface temperature increased, the pores grew steadily until the heating process was completed. Beyond that point, the pores did not continue growing, and thermal degradation took place.

In Figure 8, two transitions are shown for the temperature evolution in the samples. The first transition occurred at the beginning of the MW heating process (0–15 s). The second transition took place when water reached the boiling point (105–120 s), and the dielectric and thermal properties changed due to the presence of superheated steam. Beyond the first and the second transitions, the heating process followed a linear tendency.

SBF tests

Foams prepared with nonisolated starch mixtures from quinoa and amaranth did not retain their original shape in SBF and disintegrated in the fluid. Table II shows that the potato and sweet potato starch foams weighed in the soaked state almost seven times their weight in the dry state, whereas

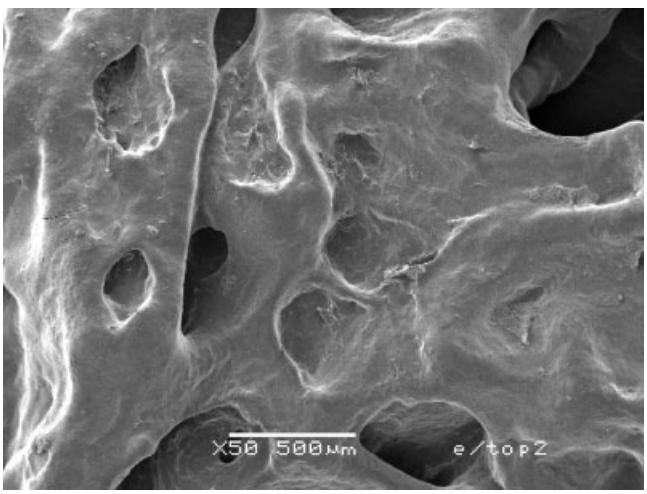

Figure 9 SEM micrograph of a 40% sweet potato starch/60% water scaffold after immersion in SBF for 21 days.

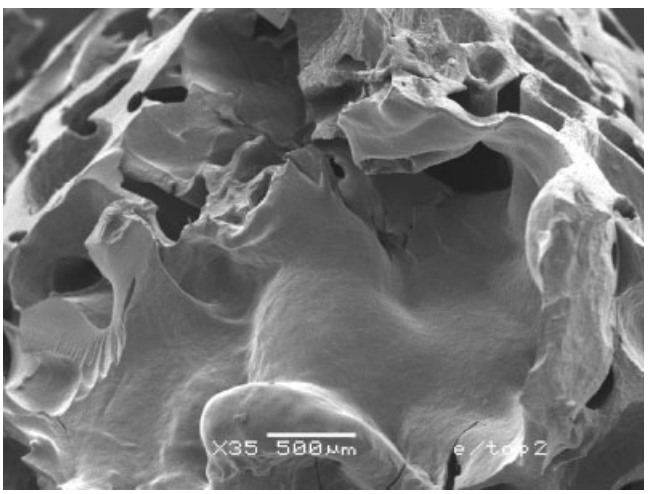

Figure 10 SEM micrograph of a 40% potato starch/60% water scaffold after immersion in SBF for 21 days.

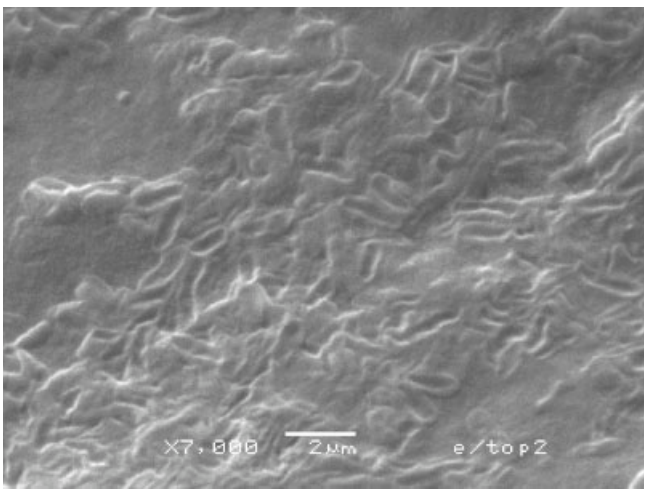

Figure 11 SEM micrograph showing the topography of an eroded 40% potato starch/60% water scaffold after immersion in SBF for 21 days.

corn samples weighed only about three times their dry weight because they had less *P*. These results confirmed the specimen's degradation after the SBF tests.

After 21 days of immersion in SBF, it appeared that there was no formation of hydroxyapatite on the surfaces of the foams. This indicated that for the material to be bioactive, the addition of inorganic fillers such as bioactive glass or hydroxyapatite might be required.[37] The SEM micrographs, as depicted in Figures 9–11, suggest that there was a change in the structure of the foams due to degradation of the polymer after 21 days of exposure in SBF, as expected.

CONCLUSIONS

MW heating was shown to be a suitable method for the production of starch-based porous structures with potential use as scaffolds for TE applications. Water was used as a blowing agent as the superheated steam left the gelatinized mixtures, and rheological properties allowed it to expand and form the final structure.

Furthermore, the scaffolds produced fulfilled the specific requirements of bone TE due to their *P*, pore size, and mechanical properties. It is accepted that for bone TE purposes, pore size should be between 200 and 900 μm.[38,39] Such values are in agreement with those obtained in this study (100–1000 μm). In addition, the indentation pressure values of the MW scaffolds (4–11 MPa), which were related to compressive strength, were also similar to the values needed for bone TE (1–10 MPa).[40]

Physical characteristics, such as pore size distribution, mean pore size, density, RWC, and *P*, depend on the source of starch used and indicate the foaming ability of the process. Sweet potato and corn starch-based scaffolds had similar physical properties to potato starch scaffolds, which showed the largest mean pore size and, therefore, the lowest densities and the highest *P* values. Mechanical properties, assessed by indentation pressure, were also related to the geometry of the pore, as the lowest indentation pressures (≈ 4 MPa) were obtained with scaffolds with highest mean pore size (≈ 880 μm).

In the SBF tests, no signs of bioactivity, characterized by the formation of hydroxyapatite layers on scaffolds surfaces, were observed.

The authors thank S. Gea of the Materials Department of Queen Mary University for experimental assistance with the DSC tests.

References

1. Lo, H.; Ponticiello, M. S.; Leong, K. W. Tissue Engineering 1995, 1, 15.
2. Whang, K.; Thomas, C. H.; Healy, K. E.; Nuber, G. Polymers 1995, 36, 837.
3. Mikos, A. G.; Thorsen, A. J.; Czerwonka, L. A.; Bao, Y.; Langer, R.; Winslow, D. N.; Vacanti, J. P. Polymer 1994, 35, 1068.
4. Lu, L.; Peter, S. J.; Lyman, M. D.; Lai, H. L.; Leite, S. M.; Tamada, J. A.; Uyama, S.; Vacanti, J. P.; Langer, R.; Mikos, A. G. Biomaterials 2000, 21, 1837.
5. Hile, D. D.; Amirpour, M. L.; Akgerman, A.; Pishko, M. V. J Controlled Release 2000, 66, 177.
6. Lu, L.; Mikos, A. G. MRS Bull 1996, 21, 28.
7. Kokubo, T.; Kushitani, H.; Sakka, S.; Kitsugi, T.; Yamamuro, T. J Biomed Mater Res 1990, 24, 721.
8. Boccaccini, A. R.; Blaker, J. J. Expert Rev Med Devices 2005, 2, 303.
9. Kokubo, T.; Takadama, H. Biomaterials 2006, 27, 2907.
10. Deporter, D. A.; Komori, N.; Howley, T. P.; Shiga, A.; Ghent, A.; Hensel, P.; Parisien, K. Calcif Tissue Int 1988, 42, 321.
11. Sachlos, E.; Reis, N.; Ainsley, B.; Derby, B.; Czermuszka, J. T. Biomaterials 2003, 24, 1487.
12. Huang, Q.; Goh, J. C.; Hutmamacher, D. W.; Lee, E. H. Tissue Eng 2002, 8, 469.
13. Haisch, A.; Loch, A.; David, J.; Pruss, A.; Hansen, R.; Sittinger, M. Med Biol Eng Comp 2000, 38, 686.
14. Zhang, M.; Haga, A.; Sekiguchi, H.; Hirano, S. Int J Biol Macromol 2000, 27, 99.
15. Salgado, A. J.; Coutinho, O. P.; Reis, R. L. Tissue Eng 2004, 10, 465.
16. Suortti, T.; Gorenstein, M. V.; Roger, P. J. Chromatogr A 1998, 828, 515.
17. Castro, J. V.; Dumas, C.; Chiou, H.; Fitzgerald, M. A.; Gilbert, R. G. Biomacromolecules 2005, 6, 2248.
18. Donald, A. M. Rep Prog Phys 1994, 57, 1081.
19. Woo, K.; Seib, P. A. Carbohydr Polym 1997, 33, 263.
20. Simkovic, I. Carbohydr Polym 1997, 34, 21.
21. Yook, C.; Pek, U. A.; Park, K. H. J Food Sci 1993, 58, 405.
22. Whistler, R.; Daniel, R. In Food Additives; Marcel Dekker: New York, 1990; p 399.
23. Sjöqvist, M.; Gatenholm, P. J Polym Environ 2005, 13, 29.

24. Malafaya, P. B.; Elvira, C.; Gallardo, A.; San Roman, J.; Reis, R. L. J Biomater Sci Polym Ed 2001, 12, 1227.
25. Souza, R. C.; Andrade, C. T. Adv Polym Tech 2002, 21, 17.
26. Stepto, R. F. T. Macromol Symp 2003, 201, 203.
27. Torres, F. G.; Díaz, R. Polym Polym Compos 2004, 12, 705.
28. Haritos, G. K.; Hager, J. W.; Amos, A. K.; Salkind, M. J.; Wang, A. S. D. Int J Solids Struct 1988, 24, 1081.
29. ASTM D2240; Standard Test Method for Rubber Property–Durometer Hardness; American Society for Testing and Materials: West Conshohocken, PA, 2005.
30. Rindlav-Westing, A.; Standing, M.; Gatenholm, P. Biomacromolecules 2002, 3, 84.
31. Gibson, L. J.; Ashley, M. F. Cellular Solids: Structure & Properties; Cambridge University Press: Cambridge, England, 1997.
32. Nelson, S.; Praskash, A.; Lawrence, K. J Microwave Power Electromagn Energy 1991, 26, 178.
33. Ryynänen, S.; Risman, P. O.; Ohlsson, T.; J Microwave Power Electromagn Energy 1995, 31, 50.
34. Bao, J.; Corke, H. J Agric Food Chem 2002, 50, 336.
35. Roushdi, M.; Harras, A.; El-Meligi, A.; Bassim, M. Starch 1983, 35, 15.
36. Galema, S. A. Chem Soc Rev 1997, 26, 233.
37. Boccaccini, A. R.; Maquet, V. Compos Sci Tech 2003, 63, 2417.
38. Yang, S.; Leong, K. F.; Du, Z.; Chua, C. K. Tissue Eng 2001, 7, 679.
39. Burg, K. J.; Porter, Kellam, J. F. Biomaterials 2000, 21, 2347.
40. Hayes, W. C.; Bouxein, M. L. In Basic Orthopaedic Biomechanics; Mow, V. C.; Hayes, W. C., Eds.; Lippincott-Raven: New York, 1997.
41. Nelson, S. O.; Lawrence, K. C.; Prakash, A. J Microwave Power 1991, 26, 178.
42. Maroulis, Z. B.; Shah, K.; Saravacos, G. D. J Food Science 1991, 56, 773.
43. Wang, L. J.; Ganjyal, G. M.; Jones, D. D.; Weller, C. L.; Hanna, M. A. Adv Polym Tech 2005, 24, 29.
44. Wilhelm, E.; Aberle, T.; Burchard, W.; Landers, R. Biomacromolecules 2002, 3, 17.
45. Ribeiro, D. M.; Corrêa, C. P.; Rodrigues, D. H.; Goneli, A. L. D.; Ciência Tecnologia Alimentos 2005, 25, 611.